agriculture

Article

Investigation of Collision Damage Mechanisms and Reduction Methods for Pod Pepper

Gaoliang Wang [1], Binghua He [2], Dianlei Han [1], He Zhang [1], Xinzhong Wang [1], Yongcheng Chen [1], Xuegeng Chen [1], Rongqiang Zhao [3,4] and Guoyu Li [5,*]

[1] School of Agricultural Engineering, Jiangsu University, Zhenjiang 212013, China; 2222116018@stmail.ujs.edu.cn (G.W.); handianlei@ujs.edu.cn (D.H.); 2212316041@stmail.ujs.edu.cn (H.Z.); xzwang@ujs.edu.cn (X.W.); yongchengchen@163.com (Y.C.); 1000005204@ujs.edu.cn (X.C.)
[2] Changyi Modern Agriculture Development Center, Changyi 261502, China; cynjj@wf.shandong.cn
[3] School of Biological and Agricultural Engineering, Jilin University, Changchun 130022, China; sharmmi@126.com
[4] Jiangsu Province and Education Ministry Co-sponsored Synergistic Innovation Center of Modern Agricultural Equipment, Zhenjiang 212013, China
[5] School of Mechanical Engineering, Shanghai Dianji University, Shanghai 201306, China
* Correspondence: ligy@sdju.edu.cn; Tel.: +86-17621342167

Abstract: This study aims to address the current situation of the late start of mechanized harvesting technology for the pod pepper, the high damage rate of existing pod pepper harvesters, and the lack of theoretical support for key harvesting components. The Hertz theory is employed to investigate the damage mechanism of collisions between pod pepper and comb fingers. The study analyzes the maximum deformation of pod pepper and the critical speed at which damage occurs during the collision process. Furthermore, it explores the critical relative speed that leads to damage in pod pepper. Orthogonal tests are conducted to analyze the effects of rotational speed, hose thickness, and moisture content on the efficiency of pod pepper picking. The experimental results are then subjected to multifactorial ANOVA to identify the optimal test parameters. The structural and motion parameters of the picking device are optimized based on these conditions. It is determined that the critical relative velocity for damage to pod pepper during a collision with the comb finger is V_0 = 11.487 m s^{-1}. The collision velocities of pod pepper with different hose thicknesses are analyzed using the i-SPEED TR endoscopic high-speed dynamic analysis system to obtain the corresponding collision velocities for different hose thicknesses. The study finds that rotational speed, hose thickness, and the water content of pod pepper affect the damage rate and stem shedding rate. The optimal experimental parameters are determined to be a rotational speed of 705.04 rpm, hose thickness of 3 mm, and water content of the pepper of 71.27%.

Keywords: comb finger; Hertz contact theory; collision speed; damage reduction methods

Citation: Wang, G.; He, B.; Han, D.; Zhang, H.; Wang, X.; Chen, Y.; Chen, X.; Zhao, R.; Li, G. Investigation of Collision Damage Mechanisms and Reduction Methods for Pod Pepper. *Agriculture* **2024**, *14*, 117. https://doi.org/10.3390/agriculture14010117

Academic Editor: Massimo Cecchini

Received: 16 December 2023
Revised: 6 January 2024
Accepted: 8 January 2024
Published: 12 January 2024

1. Introduction

Currently, the cultivation area of chili peppers in China has expanded to approximately 32 million acres, constituting over 12% of the total area dedicated to vegetable cultivation. This significant presence exemplifies the crucial role of chili peppers in China's vegetable industry [1]. Not only has the pod pepper gained popularity among domestic consumers for its distinctive flavor, but it is also known for its high vitamin C content. Vitamin C plays a vital role in promoting collagen synthesis, contributing to enhanced beauty and improved immune system function [2]. However, during mechanical harvesting, pod peppers tend to have high moisture content, making their damaged skin susceptible to discoloration, decay, or fungal growth, which affects the quality of pod pepper for storage, sale, and post-processing [3]. Consequently, this adversely impacts the storage and market value of pod peppers. Implementing low-damage pod pepper harvesters holds significant importance for fostering the growth of the pod pepper industry overall and empowering farmers to increase their income.

Due to the continuous expansion of the pod pepper cultivation area in open fields, traditional manual harvesting methods are no longer sufficient to meet the demand. In response, various chili-picking devices have been introduced in the market, such as the unfolded double helix type [4]. Kim et al. of the National Institute of Agricultural Engineering and Chonbuk National University, Korea, designed and fabricated two prototypes of an unfolded double-helix-type pepper harvester attached to a walk-behind cultivator. These two prototypes were designed and built with different frame materials, dividers, picking rollers, and auger speeds to compare the two pepper harvester field harvests [5]. The rod comb tooth type [6]: Palau et al. developed a hydraulically driven single-row pepper harvester mounted on a three-point suspension of a 35 to 45 kW tractor, which brushes the pepper from the plant by the counter-rotation of the brush drums and brushes the pepper fruits onto conveyor belts on both sides, which convey the pepper with a fan that scavenges for the magazines remaining in them. Finally, the peppers are conveyed to the hopper [7]. The strip comb finger type: Cheng et al. preferred more reasonable structural parameters and motion parameters through the construction of the test bed prototype trial production and carried out experiments of strip comb finger-type pepper picking [8]. The drum spring finger type: Qin et al. developed a new drum-spring finger-type pepper harvester. The following results were obtained through field tests on this pepper harvester: a picking rate of 99.15%, a total loss rate of 5.15%, and a breakage rate of 3.22% [9]. However, these devices primarily cater to the harvesting of plate peppers and line peppers. In the case of pod peppers, these devices still encounter certain performance issues, including a low harvesting rate and a high damage rate [10].

Currently, research on the mechanical damage of agricultural materials primarily concentrates on crops like rice, wheat, and potatoes. For instance, [11] investigated the collision damage mechanism between rice and threshing elements, while [12] explored the surface-squeezing mechanical properties and impact damage testing of Purple Cloud English Seeds. The study [13] delved into the damage mechanisms of potatoes and poles during transportation. These studies employed the Hertz contact theory to analyze the collision damage mechanism between agricultural materials and harvesting components. The findings revealed that factors such as the relative velocity of the contact point and the moisture content of the materials influence agricultural material damage. However, there is limited research on the mechanical properties of pod pepper, with emphasis primarily placed on its physical and mechanical properties, such as elastic modulus, Poisson's ratio, shear modulus, and collision coefficient. This narrow focus fails to address the research requirements of current pod pepper harvesting equipment in terms of loss reduction. Furthermore, there exists a gap in the analysis of contact mechanics and collision damage mechanisms during the picking process of pod pepper. Therefore, conducting comprehensive research on the collision damage mechanism during the picking process of pod pepper is imperative. This research not only aims to reduce the damage rate but also to ensure a high picking rate, addressing an urgent issue in need of resolution.

In this study, we aim to analyze the contact process between pod pepper and comb finger, investigate the collision damage mechanism between the two based on Hertz contact theory, and develop a model to simulate the collision between pod pepper and comb finger. We then derive equations for table deformation, surface deformation, and maximum stress distribution when the pod pepper collides with the comb finger. Additionally, we examine the critical relative velocity at which damage occurs during the collision. Through bench experiments, we analyze the impact of variables such as contact point relative velocity, flexible hose thickness, and moisture content on the collision damage experienced by pod pepper during the picking process. Furthermore, we explore methods for mitigating damage to pod pepper harvesting equipment. The findings from our study provide a theoretical foundation for optimizing the design of harvesting equipment and reducing damage to pod pepper. And the results of the study were applied to a tractor-drawn pepper harvester.

2. Materials and Methods

2.1. Mechanical Analysis of Contact between Pod Pepper and Comb Fingers

The harvesting process of the spiral comb finger-type chili harvester is as follows: A pair of spiral comb finger-type picking rollers rotate outward at the same speed. As the harvester moves, the comb fingers on the picking rollers come into contact with the chili plants, brushing against them. Due to the rotation of the picking rollers, the brushed chilies fall onto a conveyor belt. The harvested chili fruits are then transported to the aggregation device through the conveyor belt. The chilies are transferred to the feeding ports on both sides by the rotation of a spiral auger. The chilies pass through the feeding ports and collect in a material bag. After a certain period of harvesting, the material bag becomes filled with chili fruits. The chili fruits are then removed from the fixed material bag device and support frame, and a new material bag is put in place.

Analysis of the harvesting process of pod pepper shows that based on the experience of pepper harvesting, the damage in the harvesting process is mainly concentrated in the picking process, while the damage in the transportation and cleaning processes is relatively low [14–18]. The collision between pod pepper and comb fingers during the picking process can be divided into two stages: elastic deformation and damage. In order to reduce the damage rate of pod pepper during the picking process, it is necessary to control the collision between pod pepper and comb fingers in the elastic deformation stage. At this stage, the Hertz elastic contact theory can be used to calculate the deformation amount and contact stress of pod pepper and comb fingers. When the stress on pod pepper reaches the limit stress, pod pepper will be damaged or bruised. As shown in Figure 1, the damaged pod pepper will produce mold when bruised, and the skin color will change from red to black.

Figure 1. Moldy transformation in the bruises of pod peppers.

By using Hertz contact theory to analyze the collision process between pod pepper and comb fingers, the following hypothesis is proposed to simplify the calculation process [19]: During the pod pepper-picking operation, there is a continuous non-coordinated surface with comb fingers at the contact point. The maximum deformation during the collision between pod pepper and comb fingers is much smaller than the size of pod pepper, and therefore, pod pepper and comb fingers can be seen as two elastic half-spaces at the initial contact point. The contact between pod pepper and comb fingers is a collision with the center, and there is no in-plane friction during contact, so only the normal phase pressure is transmitted between the two surfaces. By analyzing the picking operation of pod pepper, a simplified schematic diagram of the collision between pod pepper and comb fingers is established, as shown in Figure 2.

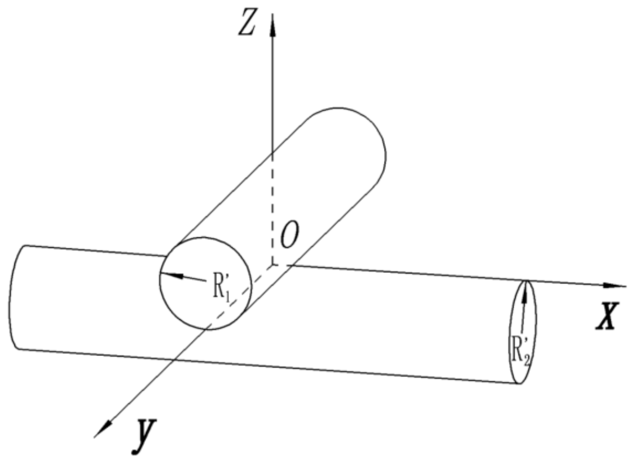

Figure 2. Schematic diagram of collision between pod pepper and comb fingers.

The contact between pod pepper and the comb finger can be analyzed using the Hertz contact theory. According to this theory, the contact area between the two objects is elliptical, with the semi-axis defined as a and b. Hertz determined that the problem of elasticity is similar to the problem of electrostatic potential. In the elliptical region of a conductor surface, the charge density changes in the longitudinal coordinate of a semi-ellipsoid, and the charge causes the potential change of the entire parabolic surface. By analogy, the distribution of pressure can be obtained. The following Equations (1)–(4), represent the elliptical size, compression amount, and maximum stress distribution of the contact area [20,21].

$$\mathrm{a} = n_a\left(\frac{3F}{2E^{*}\sum\rho}\right)^{\frac{1}{3}} \tag{1}$$

$$\mathrm{b} = n_b\left(\frac{3F}{2E^{*}\sum\rho}\right)^{\frac{1}{3}} \tag{2}$$

$$\delta = n_\delta\left(\frac{9F^2\sum\rho}{32E^{*2}}\right)^{\frac{1}{3}} \tag{3}$$

$$p_0 = \frac{3F}{2\pi ab} = \frac{1}{\pi n_a n_b}\left[\frac{3}{2}FE^{*2}\left(\sum\rho\right)^2\right]^{\frac{1}{3}} \tag{4}$$

where

a: long axis of elliptical contact area (mm);
b: short axis of elliptical contact area (mm);
δ: compression amount;
p_0: maximum stress (N);
$\sum\rho$: sum of principal curvatures; $\sum\rho = \frac{1}{R_1'} + \frac{1}{R_1''} + \frac{1}{R_2'} + \frac{1}{R_2''}$.

R_1', R_1'', R_2', R_2'': the main curvature radius of pod pepper and comb fingers at the contact point, with comb fingers made of round steel with a diameter of 6 mm, so $R_2' = 3$ mm, $R_2'' = \infty$.

E*: equivalent elastic modulus;
μ_1, μ_2, E_1, E_2: elastic modulus and Poisson's ratio of pod pepper and comb fingers;
Define $\mathrm{F}(\rho) = \frac{\left(1/R_1'' - 1/R_1'\right) + \left(1/R_2'' - 1/R_2'\right)}{\sum\rho}$.

The coefficients related to n_a, n_b, n_δ, and the principal curvature difference function F(ρ) of the contact point can be obtained by looking up the table based on F(ρ). The data not listed in the table can be obtained using interpolation method [22].

During the collision process between pod pepper and comb fingers, the deformation of the pod pepper occurs due to the compression from the comb fingers. This compression leads to a velocity difference, which can be defined as the relative velocity between the pod pepper and comb fingers. The relative velocity is described as follows:

$$V_r = V - V_p \tag{5}$$

where

V: linear speed of comb fingers (m s^{-1});
V_p: instantaneous velocity during contact between pod pepper and comb fingers (m s^{-1}).

The acceleration during the collision between pod pepper and comb fingers is as follows:

$$\frac{dV_r}{dt} = -\frac{F_t}{m} \tag{6}$$

where

F_t: instantaneous squeezing force during contact process;
m: $\frac{1}{m} = \frac{1}{m_1} + \frac{1}{m_p}$ due to $m_1 \gg m_p$, $m \approx m_p$;
m_1: quality of comb fingers (g);
m_p: quality of pod pepper (g).

Substituting Equation (4) into Equation (6) yields

$$\frac{dV_r}{dt} = -\frac{4E^*}{3m}\left(\frac{2\delta_t^3}{\sum\rho n_\delta^3}\right)^{\frac{1}{2}} \tag{7}$$

From Equation (9) transformation, it can be concluded that

$$V_r\frac{dV_r}{dt} = -\frac{4E^*}{3m}\left(\frac{2\delta_t^3}{\sum\rho n_\delta^3}\right)^{\frac{1}{2}}\frac{d\delta_t}{dt} \tag{8}$$

Align both sides simultaneously:

$$\int_0^t V_r\frac{dV_r}{dt} = \int_0^t -\frac{4E^*}{3m}\left(\frac{2\delta_t^3}{\sum\rho n_\delta^3}\right)^{\frac{1}{2}}\frac{d\delta_t}{dt} \tag{9}$$

Analyzing the contact process between pod pepper and the comb finger during the time interval: t = 0, when pod pepper comes into contact with the comb finger, F_t = 0, δ_t = 0, and V_r = V_0 (initial velocity). t = t_1, the contact between the pod pepper and the comb finger reaches maximum deformation, resulting in the maximum values of F_t and δ_t, while V_r = 0 (relative velocity becomes zero). Therefore, integrating Equation (9) over the time interval from 0 to t_1 yields

$$V_0^2 = \frac{16E^*}{15m}\left(\frac{2\delta_{max}^5}{\sum\rho n_\delta^3}\right)^{\frac{1}{2}} \tag{10}$$

In the above equation, δ_{max} is the maximum compression during the contact between pod pepper and comb finger when the stress at the contact point is maximum, so p_0 = σ_c, which is obtained by transforming Equations (3) and (4):

$$\delta_{max} = \frac{n_\delta}{2\sum\rho}\left(\frac{\pi n_a n_b \sigma_c}{E^*}\right)^2 \tag{11}$$

Substituting Equation (11) into Equation (10) yields the critical relative velocities at the time of damage produced by picking of pod pepper:

$$V_0 = \left[\frac{4n_\delta (\pi n_a n_b \sigma_c)^5}{15mE^{*4} (\sum \rho)^3} \right]^{\frac{1}{2}} \quad (12)$$

Fifty pod peppers were randomly selected from the test sample, and their size and mass were measured using dial calipers and electronic weighing equipment. The average values of these measurements were then calculated. These parameters were subsequently substituted into Equation (12) to obtain the critical relative velocity at which damage is inflicted by the collision between the pod pepper and the fingers.

2.2. Tests on the Intrinsic Parameters of Pod Pepper

The mechanical properties of pod pepper are known to be influenced by its moisture content [23,24]. However, the specific effects of different moisture contents on the mechanical properties of pod pepper have not yet been established. The current harvesting of the pod pepper is primarily performed manually, which leads to slight variations in harvest time and, consequently, in the moisture content of the harvested peppers. In order to understand the relationship between moisture content and mechanical properties, measurements were taken of the moisture content and mechanical properties of pod pepper at different maturity levels.

In order to ensure the reliability of the test, it was important to select representative pod peppers. For this purpose, the pod peppers used in the test were Tianyu pod peppers grown in the open field in Shouxian Town, Feng County, Xuzhou City, Jiangsu Province, China. This pod pepper is planted in April each year and is usually harvested by hand after ripening in October. The fruits of this pepper are ruddy and full after ripening. The pod peppers grown in this region are similar to those grown in other regions of China. In the field, we randomly collected three types of pod peppers with varying levels of maturity as our experimental samples. These samples were then stored in a crisper. Prior to conducting the experiment, we measured the moisture content of each type of pod pepper.

Prior to the experiment, we gathered 5 samples from each of the three different maturity levels of pod pepper, resulting in a total of 15 samples. For the purpose of testing the uniaxial compression mechanical properties, a cylindrical test sample of pod pepper was taken due to the irregular size of the peppers. As depicted in Figure 3, the pod pepper specimen was loaded onto the TA. XT. PLUS texture analyzer (Stable Micro Systems, Godalming, Surrey, UK) at a speed of 0.1 m/s. The tester offers a test speed range of 0.01–40 m/s, test distance accuracy of 0.001 mm, test force accuracy of 0.0002%, and traveling speed range of 0.01–40 m/s. Loading was halted upon occurrence of the pod pepper rupture. Dial calipers were employed to measure the radial deformation, while the mass tester recorded the compressive force and axial deformation curves during specimen loading. The modulus of elasticity of Asahi was calculated using Equation (13).

$$E = \frac{\sigma}{\varepsilon} \quad (13)$$

where

E: elastic modulus of pod pepper (MPa);
σ: axial compressive stress of pod pepper;
ε: axial strain of pod pepper.

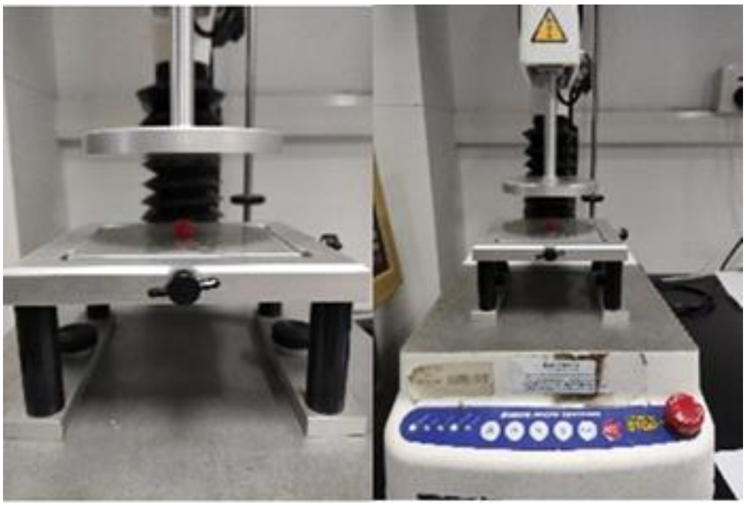

Figure 3. Experimental measurement of elastic modulus of pod pepper.

To measure the moisture content of the pod pepper, we conducted an experiment using 5 groups of pod peppers, each consisting of 10 samples, with three different maturity levels. The experiment was replicated 15 times for accuracy. As depicted in Figure 4, we utilized the DHG-9053A electric constant temperature blast drying (Zhejiang Top Cloud-Agri Technology Co., Ltd., Hangzhou, China) oven to dry the pod pepper specimens at a temperature of 105 °C for a duration of 8 h. The mass of each pod pepper specimen, denoted as m1, was recorded before the test, while the mass after drying, denoted as m_2, was measured using an electronic scale. The moisture content of the pod pepper was then calculated using Equation (14) provided below.

$$W = \frac{m_1 - m_2}{m_1} \times 100\% \tag{14}$$

where

W: moisture content of pod pepper (%);
m_1: quality of pod pepper before testing (g);
m_2: quality of pod pepper after testing (g).

(**a**) (**b**)

Figure 4. An experiment to measure the water content of peppers (**a**) in pods using a drying oven (**b**).

2.3. Picking Speed Measurement

The test equipment utilized in the experiment, as illustrated in Figure 5a, involves the measurement of the collision speed of pod peppers. The primary test equipment consists of the pod pepper collision test bench and the i-SPEED TR endoscopic high-speed dynamic analysis system (i-SPEED TR, Olympus Corporation, Tokyo, Japan). This camera is a high-speed microscope with a 1280 × 1024 pixel sensor, capable of reaching a frequency range of 24 fps to 15,000 fps. Its ultra-high sensitivity and remote-control panel CDU make the i-SPEED TR more practical. It can be used to measure distance, speed, acceleration, angular velocity, and angular acceleration, making its functions more flexible. The structure and principle of the collision test bench are as follows: the test bench features comb fingers with a diameter of 6 mm and a length of 180 mm. These comb fingers are installed on the drive shaft at 180° from each other, with a height difference of 20 mm. This configuration ensures that the collision between the pod peppercorns and the comb fingers occurs only once. Furthermore, compared to a test bench with a single comb finger, the installation of the comb fingers on the collision test bench provides more stable movement. The power element of the test bench incorporates a 4IK25RA-C speed motor, controlled by a US-52 speed controller, to facilitate different motor speeds for the pod pepper collision. The speed adjustment range spans from 90 to 1400 rpm. Additionally, the test bench employs a flexible clamping device to hold the pod peppers, allowing for an approximation of the fruit's growth on the plant. Simultaneously, this clamping device enables convenient adjustment of the pod pepper and the position where they come into contact with the comb fingers.

Figure 5. Pilgrim's collision velocimetry equipment (**a**) and flexible hoses of different thicknesses (**b**).

In the measurement of the crash velocity of the pod pepper, Figure 5b demonstrates the usage of flexible hoses with varying thicknesses. These hoses were mounted on the comb fingers during the crash testing. The pod pepper was clamped onto the crash test bench, and the rotational speed was set at 700 rpm. Throughout the crash process, the i-SPEED TR endoscopic high-speed dynamic analysis system recorded the collision at a frame rate of 1000 fps. To ensure adequate lighting for the entire filming session, fill-in lamps were utilized due to the high frame rate. The change in velocity was recorded at specific points on the pilosebaceous peppers after the collision, with the comb finger lacking the flexible hose serving as the control value. Each set of trials was repeated five times, and the results were duly recorded. The system calculated the distance covered and the time taken by the pod pepper by recording the number of pixel points traversed by the pod pepper during the collision process. Similarly, the system determined the number of pixel points occupied by the standard reference in the same plane to calculate the speed of the pod pepper during the collision process.

2.4. Crash Test of Pod Pepper

2.4.1. Theoretical Results Verification Test

Through the research on the collision damage mechanism of pod pepper, the critical relative velocity of pod pepper that produces damage is derived, and the theoretical results are verified using the pod pepper collision test bench. During the validation test, the pod pepper was placed at a position 0.15 m from the central axis to collide with the comb finger, and the critical relative velocity of the pod pepper's collision damage was known to be V_0 = 11.487 m s^{-1}, which can be calculated as the critical rotational speed of the collision experimental bench for the pod pepper's damage to be produced as n_0 = 731.29 rpm.

To ensure the accuracy of the test, several steps were taken. Firstly, the collision location between the pod pepper and the comb finger was determined by marking it with a black marker pen. This allowed for proper analysis of the post-collision results. Subsequently, the rotational speed of the crash test bench was determined based on the critical relative velocity required to cause damage. A series of tests were then conducted at various rotational speeds, specifically at 550 rpm, 600 rpm, 650 rpm, 700 rpm, 750 rpm, 800 rpm, 850 rpm, and 900 rpm, in order to examine the damage inflicted on the pod pepper at different speeds. The damage incurred by the pod pepper was categorized into fractures, breakages, and bruises. Fractures and breakages were visually identifiable, while bruises required the aid of experimental equipment for detection. The hardness change of the pod pepper was measured before and after the collision using a digital hardness tester GY-4 (Zhejiang Top Cloud-Agri Technology Co., Ltd., China) (Figure 6) to identify any bruising on the pod pepper. During the test, pod peppers with an average moisture content of 75.22% were used as test samples. At each rotational speed, the crash test was repeated three times. For each test, 300 g of pod pepper samples were removed from the crisper and securely held onto the crash test bench using a clamping device. Following each collision between the comb finger and the pod pepper, the switch was turned off, and the aforementioned steps were repeated. At the conclusion of the collision test, the damage rate of the pod pepper and the shedding rate at the fruit stalk were calculated using the following formulas:

$$\eta_p = \frac{m_1 + m_2}{m} \tag{15}$$

$$\eta_t = \frac{m_3}{m} \tag{16}$$

where

η_p: damage rate of the pod pepper (%);
η_p: shedding rate at the fruit stalk (%);
m: total mass of pod pepper specimen (g);
m_1: quality of broken and torn pilchards (g);
m_2: quality of pod pepper bruises (g);
m_3: quality of peeling at the stem of pod pepper fruit (g).

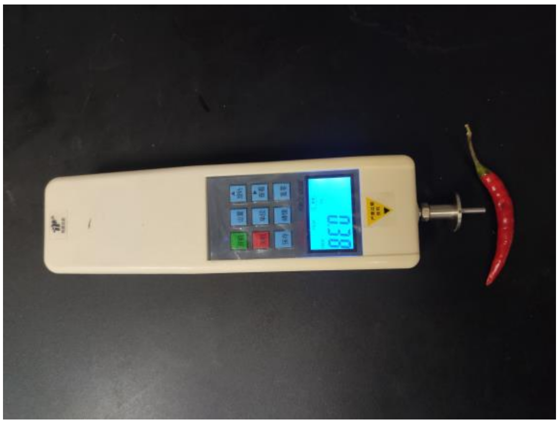

Figure 6. GY-4 digital hardness tester.

2.4.2. Material Rigidity–Flexibility Coupling Test

The study aimed to investigate the impact of rigidity–flexibility coupling materials on the damage to pod peppers. To conduct the experiments, the pod pepper crash test bench was utilized, as depicted in Figure 7a. For the experimental process, samples of pod peppers at different maturity levels were collected and depicted in Figure 7b, with respective moisture contents of 75.22%, 70.868%, and 65.943%. Additionally, flexible hoses with varying thicknesses (1 mm, 2 mm, and 3 mm) and optimized rotational speed ranges

(700 rpm, 750 rpm, and 800 rpm) were chosen. Using Design-Expert v13 software, the orthogonal experimental table was created, and collision tests were conducted on the pod pepper. Each test was repeated three times, and the average values were calculated. The damage rate of the pod peppers and the rate of peeling at the stalk were recorded. The statistical analysis used the same methodology as the collision tests described above. Furthermore, the Box–Behnken test regression model was employed to perform an ANOVA for the damage rate and the shedding rate at the stalk of the pod pepper based on the test results [25].

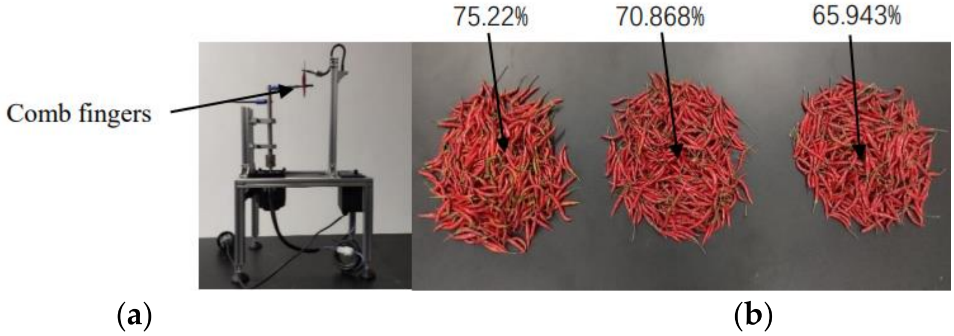

Figure 7. Material Rigidity–Flexibility coupling test bench (**a**) and pod pepper test specimen (**b**).

3. Results and Discussion

3.1. Theoretical Results Analysis

By conducting a theoretical analysis of the collision between pod pepper and comb fingers, we were able to derive the maximum deformation function (Equation (12)) and the critical relative velocity function (Equation (14)) to assess the damage inflicted on the pod pepper during the collision process. To obtain the practical result, we substituted the average values of various parameters from the measured pod pepper samples into Equation (14) and calculated that the relative speed at which the pod pepper is damaged is $V_0 = 11.487\ \mathrm{m\ s^{-1}}$.

The critical relative velocity and maximum deformation of the damage caused by the picking of pod peppers are determined by various factors, such as the modulus of elasticity, yield stress, external dimensions, quality of the pod pepper, diameter of the finger of the picking comb, material properties, and moisture content of the pod pepper. The mechanical properties of the pod pepper are directly influenced by its moisture content. The damage critical relative velocity of the pod peppers in this study was determined based on the specific test sample. However, as discussed by Cao et al., discrepancies in planting area and harvesting time can result in variations in the external dimensions and physical properties of the pod peppers [12]. Therefore, the critical relative velocity of damage to pod peppers may have some deviation. Nevertheless, the maximum deformation function (Equation (13)) and the critical relative velocity function (Equation (14)) for pod pepper damage can still be applied in the study of pod pepper damage.

3.2. Analysis of Results for Intrinsic Parameters

Based on the experimental measurements conducted, Table 1 presents the relationship between moisture content and the elastic modulus of pod pepper. From the results presented in the table, it can be concluded that there are variations in the modulus of elasticity of pod pepper at different moisture contents. Specifically, the average moisture contents for three different maturity levels of pod pepper were found to be 75.22%, 70.868%, and 65.943%. Correspondingly, the modulus of elasticity under these average moisture contents was determined to be 2.682 MPa, 2.115 MPa, and 1.712 MPa, respectively.

Upon examining the data provided in Table 1, it can be deduced that the modulus of elasticity of pod pepper exhibits an increasing trend with the rise of moisture content within the range of 65% to 75%. Therefore, the moisture content of pod pepper was selected as one of the dependent variables in the crash test, aiming to investigate its impact on the damage rate. However, it is worth noting that for cases where the moisture content was close (e.g., 73.791% and 74.907% in Table 1), the modulus of elasticity of the samples displayed a decreasing trend. This observation might be attributed to factors such as the form factor and human errors involved in measuring the modulus of elasticity of the pod peppers. To mitigate this potential error, conducting multiple experiments can yield more accurate data.

Table 1. Modulus of elasticity and water content of pod pepper.

Item	Proportion (%)	Average Ratio (%)	Variance	Modulus of Elasticity (MPa)	Average Ratio (MPa)	Variance
1	73.791 74.907 75.500 75.775 76.135	75.220	0.6727	2.652 2.538 2.582 2.763 2.876	2.682	0.0152
2	70.242 71.328 70.828 69.932 72.011	70.868	0.55752	1.936 2.182 2.103 2.079 2.275	2.115	0.0127
3	66.174 65.588 67.058 64.613 66.284	65.943	0.6615	1.746 1.579 1.791 1.607 1.835	1.712	0.0103

3.3. Analysis of Crash Velocity Results for Pod Pepper

Based on the data obtained from the i-SPEED TR endoscopic high-speed dynamic analysis system (Figure 8), variations in velocity can be observed during the impact between the pod pepper and the comb finger. The experimental results, presented in Table 2 encompass different scenarios, including collisions without a flexible hose and collisions with the inclusion of flexible hoses of various thicknesses (1 mm, 2 mm, and 3 mm). The velocities of the pilgrims after the collision were 7.656 m s^{-1}, 6.226 m s^{-1}, 5.626 m s^{-1}, and 4.66 m s^{-1}, respectively. It is important to note that the velocities measured are the average velocities during the collision, not the maximum relative velocities for the collision between the pod pepper and the comb finger.

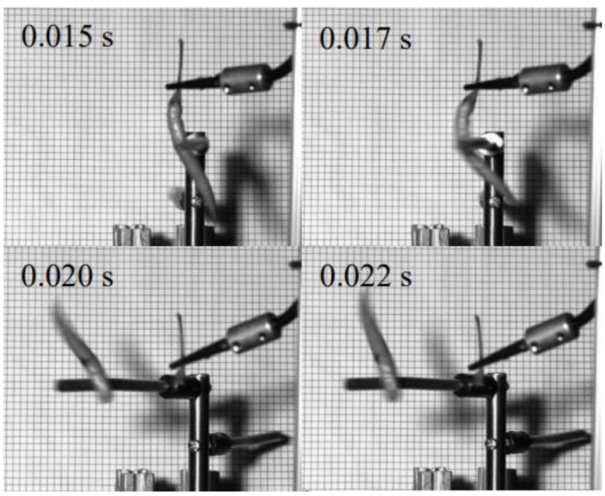

Figure 8. Change process of pod pepper during collision.

Table 2. Velocity of marked points on pod pepper after collision (m s^{-1}).

Item	1	2	3	4	5	Averages	Variance
Without hose	7.92	7.36	6.47	8.21	8.32	7.656	0.462
1 mm hose	6.03	5.72	7.00	6.48	5.90	6.226	0.213
2 mm hose	5.16	6.49	5.82	5.91	4.75	5.626	0.370
3 mm hose	4.80	5.24	3.85	4.53	4.88	4.660	0.215

Based on the data provided in Table 3, several findings can be deduced. Firstly, during the collision tests, the collision test bench exhibits a consistent rotational speed while colliding with the pod pepper. Additionally, when the comb finger is introduced along with the flexible hose, the pod pepper experiences a decrease in detachment speed following the collision. Furthermore, as the thickness of the flexible hose increases, the detachment speed of the pod pepper progressively decreases. This observation demonstrates the effectiveness of the flexible hose in reducing the impact force during the collision between the pod pepper and the comb finger. In practical applications involving the harvesting of pod peppers, minimizing the detachment speed is crucial to mitigate the risk of secondary injuries. Hence, the utilization of flexible hoses proves to be beneficial in reducing secondary collision damage to the pod peppers.

Table 3. Crash test results of pod pepper.

RPM	η_p (%)	Averages (%)	Variance	η_t (%)	Averages (%)	Variance
550	1.386 1.290 1.538	1.405	0.0104	76.530 79.162 77.940	77.877	1.1565
600	1.681 1.544 1.609	1.611	0.0031	82.407 85.391 87.434	84.744	2.9121
650	1.936 1.852 2.070	1.952	0.0081	86.237 88.350 90.142	88.243	2.5472
700	3.268 2.934 3.471	3.224	0.0490	94.38 93.258 93.357	93.357	0.2573
750	6.493 5.916 5.637	6.015	0.1270	95.718 95.524 96.700	95.981	0.2650
800	7.934 8.316 8.703	8.317	0.0986	94.490 96.524 96.941	95.985	1.1464
850	10.317 10.152 9.915	10.128	0.0272	97.138 97.060 95.943	96.714	0.2980
900	11.749 12.327 13.061	12.379	0.2882	95.726 96.640 97.972	96.779	0.8505

3.4. Analysis of Crash Test Results of Pod Pepper

3.4.1. Analysis of Theoretical Validation Test Results

By adjusting the pod pepper collision test bench, the comb fingers were made to collide with the pod pepper at different rotational speeds. As shown in Figure 9, the breaks, breakage, and bruising of the pod pepper in the collision test were recorded. At the end of the crash test of pod peppers, we counted the quality of breaks, breakage, bruising and shedding at the stalk of pod peppers. Through calculation, the damage rate and the shedding rate at the stalk of pod pepper were obtained. The specific test results are shown in Table 2.

Figure 9. Breaks, breakage, and bruising of pilosebaceous peppers in the pilosebaceous crash test.

Upon analyzing Table 3, several insights can be gleaned. When the rotational speed of the crash test bench is below the critical speed of 731.29 rpm for pod pepper damage, some degree of damage still occurs, but at a rate lower than 3.224%. Apart from factors such as the modulus of elasticity, yield stress, external dimensions, quality, and diameter and material of the picking comb fingers, there are additional influencing factors. However, these other factors show minimal impact on the damage rate of the pod pepper when the rotational speed is below the critical threshold. Comparing the damage rates, the increase in the damage rate from a rotational speed of 650 rpm to 700 rpm is significantly smaller than the increase from 700 rpm to 750 rpm. Nonetheless, a small discrepancy remains between the critical relative velocities of actual pod pepper collision damage and the theoretically calculated values. This discrepancy may be attributed to several factors. Firstly, the Hertz elastic contact theory analysis is based on assumptions and does not fully account for the complex actual contact process between the pod pepper and the comb finger, resulting in potential errors in theoretical calculations. Secondly, the irregular size and shape of the pod pepper often necessitate the use of average values in theoretical calculations, which could introduce errors in the calculation results. Lastly, variations in the ripeness and moisture content of the peppers may also influence experimental results by altering the physical properties and mechanical behavior of the pod pepper. Although some disparities exist between the theoretically calculated and experimental values of the contact mechanics between the pod pepper and comb fingers, these differences fall within an acceptable range. Consequently, the theoretical model of the collision between the pod pepper and comb fingers can be used as a reference in guiding the design of structural and kinematic parameters for the pod pepper harvester.

As observed from the shedding rate at the stalk of the pod peppers in Table 3, when the rotational speed of the crash test bench exceeded 750 rpm, the shedding rate at the stalk remained approximately 95%, but there was a significant increase in the damage rate. To achieve a higher picking rate and minimize damage to the pod peppers, the following measures can be implemented: Firstly, increasing the rotational speed of the pod peppers during picking can be effective. Additionally, utilizing damage reduction methods can help decrease the damage rate of the pod peppers. By implementing these strategies, both the picking rate and the damage rate of the pod pepper-picking operation can meet the industry standard.

3.4.2. Analysis of the Results of the Material Rigidity–Flexibility Coupling Test

Upon analyzing the speed variations of flexible hoses with varying thicknesses on the pod pepper after the collision, it can be concluded that the thickness of the flexible hoses has an impact on the collision damage to the pod pepper. Consequently, for orthogonal experiments, we selected the water content of the pod pepper, the thickness of the flexible hose, and the rotational speed of the collision experimental table as the influential factors.

The experimental results, presented in Table 4, utilize the damage rate of the pod pepper and the shedding rate at the stalk as evaluation criteria.

Table 4. Results of collision orthogonal test of pod pepper.

Item	RPM	Hose Thickness (mm)	Water Content (%)	η_p (%)	η_t (%)
1	700	1	70.868	2.34	90.93
2	750	2	70.868	2.63	95.14
3	800	2	75.22	5.81	95.94
4	700	3	70.868	1.23	88.31
5	700	2	75.22	1.98	88.75
6	700	2	65.943	1.78	89.96
7	750	3	75.22	2.35	94.08
8	800	3	70.868	3.43	96.23
9	750	2	70.868	2.47	95.33
10	800	2	65.943	4.08	97.83
11	750	2	70.868	2.74	94.08
12	750	2	70.868	2.18	95.29
13	750	1	75.22	3.94	94.91
14	750	1	65.943	3.26	96.82
15	750	2	70.868	2.57	95.63
16	800	1	70.868	6.17	96.52
17	750	3	65.943	2.05	95.38

The orthogonal test results were analyzed using Design-Expert 13 software based on the data presented in Table 5. The analysis of variance was performed using the Box–Behnken test regression model for the damage rate of the pod pepper. The relevant results are shown in Table 5. Upon analyzing the results in the table, it can be observed that the *p*-value of the model is less than 0.0001, while the *p*-value of the misfit value is greater than 0.05. This suggests that the model is highly significant and that the regression model exhibits a strong degree of fit. Additionally, by examining the *p*-values of the rotational speed of the crash test bench, the thickness of the flexible hose, and the water content of the pod pepper, it can be determined that all three factors have a highly significant effect on the damage rate of the pod pepper. Moreover, the effects of the rotational speed of the crash test bench and the thickness of the flexible hose on the damage rate of the pod pepper are more pronounced compared to the effect of the water content of the pod pepper.

Table 5. Results of analysis of variance (ANOVA) for damage rate of pod pepper.

Source	Sum of Squares	DF	F-Value	*p*-Value
Model	28.58	9	51.69	<0.0001
RPM	16.27	1	264.82	<0.0001
Hose Thickness	5.07	1	82.50	<0.0001
Water Content	0.64	1	10.39	0.00146
Residual	0.4301	7		
Lack of Fit	0.2490	3	1.83	0.2812
Pure Error	0.1811	4		
Cor Total	29.01	16		

Note: RPM, Revolutions Per Minute; DF, Degree Freedom.

Based on the data shown in Table 6, we can see that for the shedding rate at the stalk of the pod pepper, the Box–Behnken test regression model was used to analyze the ANOVA. The results showed that the *p*-value of the model for the abscission rate was less than 0.05, which means that the regression model was highly significant. On the other hand, the *p*-value of the misfit term was greater than 0.05, indicating that the model was not significantly misfitted. Based on the *p*-values in the table, it can be concluded that the rotational speed of the crash test bench, the thickness of the flexible hose, and the moisture content of the pod pepper had a highly significant effect on the breakage of the pod pepper fruit stalks. Meanwhile, the collision test bench rotational speed had the greatest effect on the shedding of the fruit stalks of pod pepper, while the water content had the least effect.

Table 6. Results of analysis of variance (ANOVA) for the rate of abscission at the petiole of pod peppers.

Model	Sum of Squares	DF	F-Value	*p*-Value
RPM	131.20	9	58.17	<0.0001
Hose Thickness	98.84	1	394.41	<0.0001
Water Content	3.43	1	13.69	0.0077
Residual	4.91	1	19.58	0.0031
Lack of Fit	1.75	7		
Pure Error	0.3425	3	0.3235	0.8096
Cor Total	1.41	4		
Model	132.95	16		

Note: RPM, Revolutions Per Minute; DF, Degree Freedom.

The interaction effects of the factors were visually depicted through the generation of 3D response surface plots using Design-Expert 13 software. These plots provide a more intuitive representation of the effects of the factors on the damage rate and the rate of abscission at the stalk of the pod pepper. The analysis of variance results presented in Tables 3 and 4 indicate that the crash test bench rotational speed and flexible hose thickness exerted significantly greater effects on the damage rate and shedding rate of the fruit stalks of the pod pepper compared to the water content of the pod pepper. Consequently, response surfaces depicting the influence of the crash test bench rotational speed and flexible hose thickness on the damage rate and stalk shedding rate of pod peppers were established (Figure 10a,b). In Figure 10a, it is evident that an increase in the rotational speed of the crash test bench leads to a corresponding increase in the damage rate of the pod pepper. Conversely, an increase in the thickness of the hose results in a decrease in the damage rate. The minimum damage rate of the pod pepper occurs when the rotational speed is at its minimum value and the hose thickness is at its maximum value. Figure 10b demonstrates that an increase in the thickness of the flexible hose leads to a decrease in the shedding rate at the stem of the pod pepper while an increase in the rotational speed.

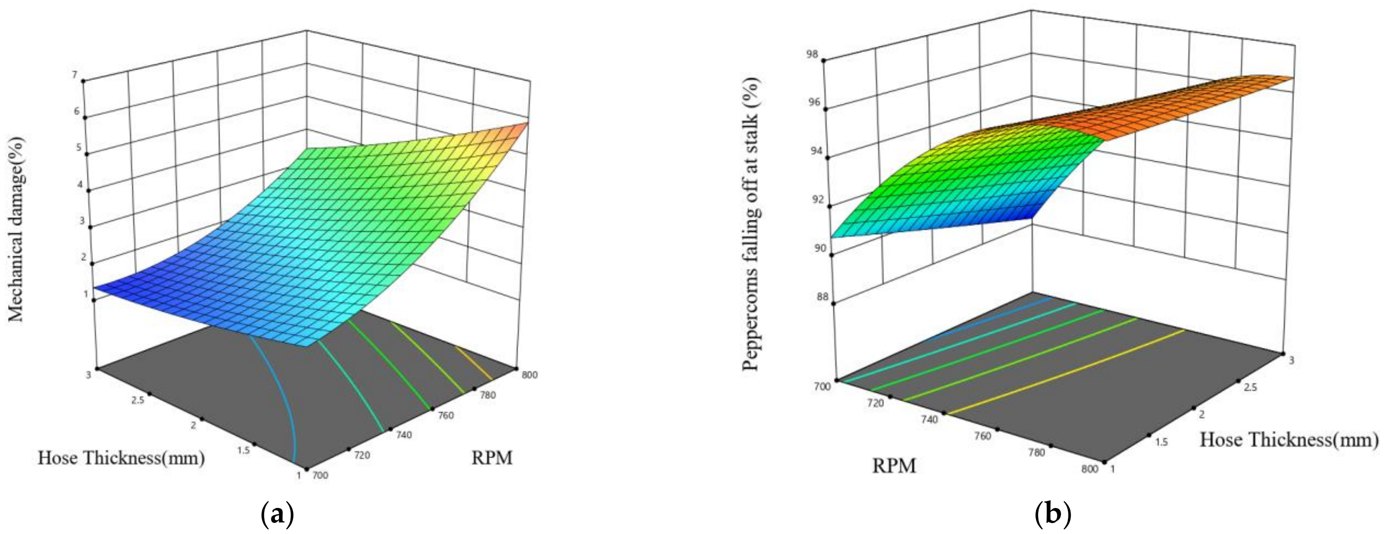

Figure 10. Interactive corresponding surface analysis results. (**a**) The influence of RPM and Hose Thickness on the Mechanical damage; (**b**) The influence of RPM and Hose Thickness on the Peppercoms falling off at stalk.

For the regression models of the damage rate and the shedding rate at the stalk of pod pepper, we used the optimization function of the Design-Expert 13 software to solve for the optimal rotation speed of the crash test bench, the thickness of the flexible hose, and the harvested moisture content of the pod pepper. With a minimum damage rate of 1.23% for pod pepper and a maximum shedding rate of 97.83% at the stalk, we obtained the following optimal experimental parameters: the speed of the crash test bench was 705.04 rpm, the thickness of the flexible hose was 3 mm, and the water content of the pod peppers was 71.27%.

Theoretical analyses and bench tests are all aimed at frontal collision studies between pod peppers and comb fingers. However, in actual pod pepper-picking operations, the collision between comb fingers and pod peppers is complex and varied, and there may be multiple collisions between multiple comb fingers and pod peppers, which can lead to differences in the damage rate of pod peppers. Nevertheless, the results of the theoretical analysis and the bench test are similar, which indicates that the test results can be used in the research of the pod pepper-picking device. In response to a previous study, Duan et al. analyzed the damage mechanism of the pepper-picking process by means of a high-speed camera to optimize the motion parameters of the pepper-picking device [3]. However, the article investigated the collision damage mechanism between the pod pepper and comb finger through the Hertz contact theory and analyzed the effects of rotational speed, material rigid–flexible coupling, and moisture content on the picking damage to pod pepper through an orthogonal test. The research in this article can optimize the structural parameters and motion parameters of the picking device and reduce the damage rate of the picking process to pod pepper from various aspects.

4. Conclusions

(1) Substituting each parameter of the test sample of pod pepper into the critical velocity function, V_0 = 11.487 m s^{-1} was obtained.

(2) The average moisture content of pod pepper was 75.22%, 70.868%, and 65.943%, while the average values of its elastic modulus at the corresponding moisture content were 2.682 MPa, 2.115 MPa, and 1.712 MPa. It can be seen that the elastic modulus of pod pepper increased with the increase in moisture content.

(3) Research on hoses of different thicknesses found that the speed of pod pepper collisions gradually decreased with the increase in the thickness of the flexible hose. According to the experimental results, the average values of the collision speed corresponding to different thicknesses of hose are as follows: no hose (7.656 m s^{-1}), 1 mm flexible hose (6.226 m s^{-1}), 2 mm hose (5.626 m s^{-1}), 3 mm hose (4.66 m s^{-1}).

(4) The reliability of the theoretical results was verified by the crash test bench. In the research results, the impact of three factors on the damage rate to the pod peppers is listed in descending order: rotational speed, hose thickness, and moisture content. The impact of three factors on the rate of stem shedding in pod chili peppers, from highest to lowest, is as follows: rotational speed, thickness of the hose, and moisture content in pod chili peppers. This study determined the optimal experimental parameters for the harvesting process of the pod pepper, with a rotational speed of 705.04 rpm, a hose thickness of 3 mm, and a moisture content of 71.27%. The research results are of great significance for improving the structural parameters and motion parameters of the pod pepper harvester and increasing the income of farmers in planting pod peppers. These results are also of great significance for in-depth research on the pod pepper-harvesting device in the future.

Author Contributions: Conceptualization, X.C. and Y.C.; methodology, Y.C. and B.H.; software, G.W.; validation, H.Z., Y.C. and R.Z.; formal analysis, Y.C.; investigation, D.H.; resources, X.W. and B.H.; data curation, G.W. and B.H.; writing—original draft preparation, G.W.; writing—review and editing, G.L. and B.H.; visualization, H.Z.; supervision, D.H.; project administration, X.W.; funding acquisition, G.L. All authors have read and agreed to the published version of the manuscript.

Funding: This work was supported by the Jiangsu Province Modern Agricultural Machinery Equipment and Technology Demonstration and Extension Project (NJ2020-14), Jiangsu Province and Education Ministry Co-sponsored Synergistic Innovation Center of Modern Agricultural Equipment (No. XTCX2003), the National Key Research and Development Project (No. 2022YFD2002403), the Priority Academic Program Development of Jiangsu Higher Education Institutions (No. PAPD-2018-87), the National Natural Science Foundation of China (No. 52105304), and the "Doctor of Innovation and Entrepreneurship" Project of Jiangsu Province (No. JSSCBS20210939).

Institutional Review Board Statement: Not applicable.

Data Availability Statement: The datasets used and/or analyzed during the current study are available from the corresponding author upon reasonable request.

Conflicts of Interest: The authors declare that they have no known competing financial interests or personal relationships that could have appeared to influence the work reported in this paper.

References

1. Lin, Q.; Xin, Z.; Kong, L.; Wang, X.; Yang, X.; He, W. Current situation of pepper industry development and breeding countermeasures in China. *J. China Agric. Univ.* **2023**, *28*, 82–95.
2. Azlan, A.; Sultana, S.; Huei, C.S.; Razman, M.R. Antioxidant, Anti-Obesity, Nutritional and Other Beneficial Effects of Different Chili Pepper: A Review. *Molecules* **2022**, *27*, 898. [CrossRef] [PubMed]
3. Duan, Y.; Kong, L.; Cheng, Y. Tine drum pepper picking device picking hot pepper mechanical damage characteristic and mechanism. *Trans. Chin. Soc. Agric. Mach.* **2014**, *35*, 79–82. [CrossRef]
4. Nam, J.N.; Byun, J.; Kim, T.; Kim, M.; Kim, D. Measurement of Mechanical and Physical Properties of Pepper for Particle Behavior Analysis. *J. Biosyst. Eng.* **2018**, *43*, 173–184.
5. Kim, T.H.; Kim, D.C.; Cho, Y. Performance Comparison and Evaluation of Two Small Chilli Pepper Harvester Prototypes That Attach to Walking Cultivators. *Appl. Sci.* **2020**, *10*, 2570. [CrossRef]
6. Funk, P.A.; Walker, S.J. Evaluation of Five Green Chile Cultivars Utilizing Five Different Harvest Mechanisms. *Appl. Eng. Agric.* **2010**, *26*, 955–964. [CrossRef]
7. Palau, E.; Torregrosa, A. Mechanical harvesting of Paprika peppers in Spain. *J. Agric. Eng. Res.* **1997**, *66*, 195–201. [CrossRef]
8. Cheng, Y.; Hu, S.; Yuan, Y. Research of comb-type picking device for chilli peppers. In Proceedings of the 2012 International Academic Annual Conference of China Agricultural Machinery Society, Hangzhou, China, 20 October 2012; pp. 942–948.
9. Qin, X.; Lei, J.; Chen, Y. Design and research on key components of a novel self-propelled chili pepper harvester. *Adv. Mater. Res.* **2012**, *468–471*, 794–797. [CrossRef]
10. Du, C.; Han, D.; Song, Z.; Chen, Y.; Wang, X. Calibration of contact parameters for complex shaped fruits based on discrete element method: The case of pod pepper (*Capsicum annuum*). *Biosyst. Eng.* **2023**, *226*, 43–54. [CrossRef]
11. Xu, L.; Li, Y. Critical speed of impact damage on a rice kernel. *Nongye Jixie Xuebao/Trans. Chin. Soc. Agric. Mach.* **2009**, *40*, 54–57.
12. Cao, M.; Gao, X.; Wang, J.; You, Z.; Wu, H.; Wang, G. Research on mechanical properties and threshing-impact damage of Astragalus sinicus seeds. *J. Chin. Agric. Mech.* **2022**, *43*, 77. [CrossRef]
13. Liang, Z.; Huang, Y.; Li, D.; Wada, M.E. Parameter determination of a viscoelastic–plastic contact model for potatoes during transient collisions. *Biosyst. Eng.* **2023**, *234*, 156–171. [CrossRef]
14. Yuan, X.; Yang, S.; Jin, R.; Zhao, L.; Dao, E.; Zheng, N.; Fu, W. Design and experiment of double helix pair roller pepper harvesting device. *Trans. Chin. Soc. Agric. Eng.* **2021**, *37*, 1. [CrossRef]
15. Wall, M.M.; Walker, S.; Wall, A.D.; Hughs, E.; Phillips, R. Yield and quality of machine harvested red chile peppers. *HortTechnology* **2003**, *13*, 296–302. [CrossRef]
16. Kang, K.-S.; Park, H.-S.; Park, S.-J.; Kang, Y.-S.; Kim, D.-C. Study on Optimal Working Conditions for Picking Head of Self-Propelled Pepper Harvester by Factorial Test. *J. Biosyst. Eng.* **2016**, *41*, 12–20. [CrossRef]
17. Stanly, N.M.; Jayan, P.R.; Malkani, P.; Wankhade, R.D. Designe and Development and Evaluation of Pepper Harvester. *J. AgriSearch* **2020**, *6*, 82–85. [CrossRef]
18. Gupta, C.; Tewari, V.K.; Machavaram, R. Evaluation of a Laboratory-based Prototype of a Comb-type Picking Mechanism for Chili Pepper Harvester. *J. Biosyst. Eng.* **2022**, *47*, 69–78. [CrossRef]
19. Popov, V.L. Contact mechanics and friction: Physical principles and applications, second edition. In *Contact Mechanics and Friction: Physical Principles and Applications*, 2nd ed.; Springer: Berlin/Heidelberg, Germany, 2017. [CrossRef]
20. Shull, K.R. *Elastomer Surfaces, Contact Mechanics Testing of Encyclopedia of Materials: Science and Technology*; Buschow, K.H.J., Cahn, R.W., Flemings, M.C., Eds.; Elsevier: Oxford, UK, 2001; pp. 2449–2451.
21. Sitkei, G. *Mechanics of Agricultural Materials*; Elsevier Science Publishers: Amsterdam, The Netherlands, 1986.
22. Deng, S.; Jia, Q.; Xue, J. *Principles of Rolling Bearing Design*, 2nd ed.; China Standard Press: Beijing, China, 2014; Chapter 5.

23. Physical properties of plant and animal materials. *J. Agric. Eng. Res.* **1968**, *13*, 379. [CrossRef]
24. Li, Y.; Wang, X.; Xu, L.; Chen, J. Study on compression properties of rice grains. *Nongye Jixie Xuebao/Trans. Chin. Soc. Agric. Mach.* **2007**, *38*, 56–59.
25. Bazaria, B.; Kumar, P. Optimization of spray drying parameters for beetroot juice powder using response surface methodology (RSM). *J. Saudi Soc. Agric. Sci.* **2018**, *17*, 408–415. [CrossRef]